ISSN 1392–1207. MECHANIKA. 2020 Volume 26(5): 390–397

Adaptive Powell's Identification of Elastic Constants of Composite Glass Girder with Layered Shell Element Theory

Jian ZHANG*, Yanlong JIANG, Wei SUN***, Hua LIU****, Guodong LI*****, Jiayong WANG********

**Nanjing University of Aeronautics and Astronautics, 210016 Nanjing, China, E-mail: jianzhang78@126.com (Corresponding Author)*

***Nanjing University of Aeronautics and Astronautics, 210016 Nanjing, China, E-mail: jiangyan-long@nuaa.edu.cn*

****Nanjing University of Aeronautics and Astronautics, 210016 Nanjing, China, E-mail: nancysun@nuaa.edu.cn*

*****China Railway Major Bridge (Nanjing) Bridge and Tunnel Inspect and Retrofit Co., Ltd., 210031 Nanjing, China, E-mail: kylinbridge@163.com*

******STECOL Corporation, 300384 Tianjing, China, E-mail: liguodong@163.com*

*******STECOL Corporation, 300384 Tianjing, China, E-mail: wangjiayong@126.com*

crossref http://dx.doi.org/10.5755/j01.mech.26.5.27873

1. Introduction

Box-section girder bridge refers to the girder bridge whose main girder is in the form of thin-walled closed cross-section. Usually, long hollow trusses made of steel or concrete are used as girders, which makes the bridge light and strong [1-3]. Bridges built in this way are called box girder bridges and with the improvement of bridge technology in China, the aesthetics of bridges is getting higher and higher [4-5]. Cast-in-situ continuous box girder plays an important role in bridge construction because of its simple shape, beautiful appearance, large torsional stiffness, good integrity and strong applicability [6-8]. Because of the complexity of box girder problems, domestic research is not fully mature, and the overall design ideas of each unit are also different, which leads to the diversity of design drawings of cast-in-place box girder. Two or more spans of continuous box girder bridges belong to statically indeterminate system [9-11]. Under the action of constant live load, the negative bending moment of fulcrum produced by continuous beam has unloading effect on the positive bending moment in midspan, which makes the internal force state more uniform and reasonable, so that the beam height can be reduced, thus the clearance under bridge can be increased, the material can be saved, and the stiffness is large, the integrity is good, the overloading capacity is large, the safety is large, and the expansion joint of bridge deck is small [12-13]. Because the bending moment of mid-span section decreases, the bridge span can be increased. Even so, in the mechanical analysis of box girder structure, the elastic constants of the structure must be known, otherwise the structural analysis can not continue [14-15]. The main methods of mastering structural elastic constants are mainly divided into laboratory experimental analysis and numerical back analysis, while the former can not reflect the actual working environment of the structure and other factors. Therefore, this paper takes composite glass girders as the research object, and studies how to accurately determine the elastic constants of composite glass girders by numerical back analysis method.

Thus, the layered shell element for the composite glass girder structure is analyzed and the generalized Bayesian objective function of elastic constants of the girder is deduced. Then, the adaptive Powell's identification model for the elastic constants is founded. Finally, through classic examples, some regularities of adaptive Powell's identification of elastic constants are deeply probed into.

2. Generalized Bayesian objective function of elastic constants of composite glass box girder

In the process of adaptive Powell's identification of the elastic constants of composite glass box structure, the elastic constants can be treated as random variables noted as the random vector $\boldsymbol{Z}=[z_1\ z_2\ \cdots\ z_m]^{\mathrm{T}}$ (m is the dimension of the vector $\boldsymbol{Z}$) to put the identification of the elastic constants into execution [16-18]. From Bayesian estimation theory, it can be noted as:

$$f(\boldsymbol{Z}\,|\,\boldsymbol{W}^*)=\frac{f(\boldsymbol{W}^*\,|\,\boldsymbol{Z})f(\boldsymbol{Z})}{f(\boldsymbol{W}^*)}, \tag{1}$$

where: $f(\boldsymbol{Z})$ is the priori information distribution of the systematic constant; $f(\boldsymbol{W}^*\,|\,\boldsymbol{Z})$ is the conditional distribution of the systematic response; $f(\boldsymbol{W}^*)$ is the systematic response distribution; $f(\boldsymbol{Z}\,|\,\boldsymbol{W}^*)$ is the posterior information distribution. Presuming the elastic constants $\boldsymbol{Z}$ are conformed to Gaussian normal distribution, the priori information distribution $f(\boldsymbol{Z})$ is expressed as:

$$f(\boldsymbol{Z})=(2\pi)^{-\frac{m}{2}}\left|\boldsymbol{C}_Z\right|^{-1}\times \\ \times exp\left[-\frac{1}{2}(\boldsymbol{Z}-\boldsymbol{Z}_0)^T\boldsymbol{C}_Z^{-1}(\boldsymbol{Z}-\boldsymbol{Z}_0)\right], \tag{2}$$

where: $\boldsymbol{Z}_0$ is the expectation vector and $\boldsymbol{C}_z$ is the covariance matrix of the elastic constants $\boldsymbol{Z}$ of composite glass box girder.

If the ordinary Bayesian objective function is used to identify the elastic constants $\boldsymbol{Z}$ of the composite glass box girder, there is much repeated and worthless work [19-21]. Thus the generalized Bayesian objective function of the elastic constants is deduced. Supposing that n is the times of measured systematic response data, $\prod_{i=1}^{n} f(\boldsymbol{W}_i^* \mid \boldsymbol{Z})$ is called the united density function of $\boldsymbol{W}_i^*$ and then defining the systematic response vector of the computational results as $\boldsymbol{W}_i = \boldsymbol{W}_i(\boldsymbol{Z})$, the former united density function is also derived as:

$$f(\boldsymbol{W}^* \mid \boldsymbol{Z}) = (2\pi)^{-\frac{mn}{2}} \prod_{i=1}^{n} \left| \boldsymbol{C}_{\boldsymbol{W}_i^*} \right|^{-1} \times \\ \times \exp\left[-\frac{1}{2} \sum_{i=1}^{n} (\boldsymbol{W}_i^* - \boldsymbol{W}_i)^{\mathrm{T}} \boldsymbol{C}_{\boldsymbol{W}_i^*}^{-1} (\boldsymbol{W}_i^* - \boldsymbol{W}_i) \right], \tag{3}$$

Substituting Eqs. (2-3) into Eq. (1), the generalized Bayesian objective function J and the partial differentiation of the function J to the elastic constants $\boldsymbol{Z}$ are finally obtained as:

$$J = \sum_{i=1}^{n} (\boldsymbol{W}_i^* - \boldsymbol{W}_i)^{\mathrm{T}} \boldsymbol{C}_{\boldsymbol{W}_i^*}^{-1} (\boldsymbol{W}_i^* - \boldsymbol{W}_i) + \\ +(\boldsymbol{Z} - \boldsymbol{Z}_0)^{\mathrm{T}} \boldsymbol{C}_{\boldsymbol{Z}}^{-1} (\boldsymbol{Z} - \boldsymbol{Z}_0), \tag{4}$$

$$\frac{\partial J}{\partial \boldsymbol{Z}} = \sum_{i=1}^{n} 2 \left(\frac{\partial \boldsymbol{W}_i}{\partial \boldsymbol{Z}} \right)^{\mathrm{T}} \boldsymbol{C}_{\boldsymbol{W}_i^*}^{-1} (\boldsymbol{W}_i - \boldsymbol{W}_i^*) + \\ +2\boldsymbol{C}_{\boldsymbol{Z}}^{-1} (\boldsymbol{Z} - \boldsymbol{Z}_0). \tag{5}$$

When $\boldsymbol{W}_i(\boldsymbol{Z})$ is submitted with Taylor formula expansion at the expectation point $\boldsymbol{Z}$ and only the first two items are reserved, it is derived as:

$$\boldsymbol{W}_i(\boldsymbol{Z}) = \boldsymbol{W}_i(\overline{\boldsymbol{Z}}) + \boldsymbol{S}_i(\overline{\boldsymbol{Z}})(\boldsymbol{Z} - \overline{\boldsymbol{Z}}), \tag{6}$$

where: $\boldsymbol{S}_i(\overline{\boldsymbol{Z}}) = \left. \frac{\partial \boldsymbol{W}_i}{\partial \boldsymbol{Z}} \right|_{\boldsymbol{Z}=\overline{\boldsymbol{Z}}}$ is called the sensitivity matrix. Substituting Eq. (6) into Eq. (5), it can be obtained as:

$$\frac{\partial J}{\partial \boldsymbol{Z}} = \sum_{i=1}^{n} 2\boldsymbol{S}_i^{\mathrm{T}} \boldsymbol{C}_{\boldsymbol{W}_i^*}^{-1} (\overline{\boldsymbol{W}}_i + \boldsymbol{S}_i \boldsymbol{Z} - \boldsymbol{S}_i \overline{\boldsymbol{Z}} - \boldsymbol{W}_i^*) + \\ +2\boldsymbol{C}_{\boldsymbol{Z}}^{-1} (\boldsymbol{Z} - \boldsymbol{Z}_0), \tag{7}$$

where: $\overline{\boldsymbol{W}}_i = \boldsymbol{W}_i(\overline{\boldsymbol{Z}})$. Letting Eq. (7) equal to zero, it is achieved as:

$$\left[\sum_{i=1}^{n} \boldsymbol{S}_i^{\mathrm{T}} \boldsymbol{C}_{\boldsymbol{W}_i^*}^{-1} \boldsymbol{S}_i + \boldsymbol{C}_{\boldsymbol{Z}}^{-1} \right] \boldsymbol{Z} = \\ = \sum_{i=1}^{n} \boldsymbol{S}_i^{\mathrm{T}} \boldsymbol{C}_{\boldsymbol{W}_i^*}^{-1} (\boldsymbol{W}_i^* - \overline{\boldsymbol{W}}_i + \boldsymbol{S}_i \overline{\boldsymbol{Z}}) + \boldsymbol{C}_{\boldsymbol{Z}}^{-1} \boldsymbol{Z}_0. \tag{8}$$

Assuming $\boldsymbol{H} = \sum_{i=1}^{n} \boldsymbol{S}_i^{\mathrm{T}} \boldsymbol{C}_{\boldsymbol{W}_i^*}^{-1} \boldsymbol{S}_i + \boldsymbol{C}_{\boldsymbol{Z}}^{-1}$ and $\boldsymbol{M} = \boldsymbol{H}^{-1} \left[\boldsymbol{S}_1^{\mathrm{T}} \boldsymbol{C}_{\boldsymbol{W}_1^*}^{-1}, \boldsymbol{S}_2^{\mathrm{T}} \boldsymbol{C}_{\boldsymbol{W}_2^*}^{-1}, \cdots, \boldsymbol{S}_n^{\mathrm{T}} \boldsymbol{C}_{\boldsymbol{W}_n^*}^{-1} \right]$, from Eq. (8) the identification value $\hat{\boldsymbol{Z}}$ of the elastic constants $\boldsymbol{Z}$ of the composite glass box structure can be noted as:

$$\hat{\boldsymbol{Z}} = (\boldsymbol{I} - \boldsymbol{M}\boldsymbol{S})\boldsymbol{Z}_0 + \boldsymbol{M}\boldsymbol{W}^* - \boldsymbol{M}(\overline{\boldsymbol{W}} - \boldsymbol{S}\overline{\boldsymbol{Z}}), \tag{9}$$

where: $\overline{\boldsymbol{W}} = \left[\overline{\boldsymbol{W}}_1, \overline{\boldsymbol{W}}_2, \cdots, \overline{\boldsymbol{W}}_n \right]^{\mathrm{T}}$ and $\overline{\boldsymbol{W}}_i$ is the systematic response vector of the i th computational data at the expectation point $\overline{\boldsymbol{Z}}$. $\boldsymbol{W}^* = \left[\boldsymbol{W}_1^*, \boldsymbol{W}_2^*, \cdots, \boldsymbol{W}_n^* \right]^{\mathrm{T}}$ and $\boldsymbol{W}_i^*$ is the vector of the i th measured systematic response data. $\boldsymbol{S} = \left[\boldsymbol{S}_1, \boldsymbol{S}_2, \cdots, \boldsymbol{S}_n \right]^{\mathrm{T}}$ and $\boldsymbol{S}_i$ is the sensitivity matrix of the i th measured systematic responses. And $\boldsymbol{I}$ is a unit matrix. Assuming the priori information $\boldsymbol{Z}_0$ of the elastic constants $\boldsymbol{Z}$ of the composite glass box structure is irrelative with the measured systematic response data $\boldsymbol{W}^*$, from Eq. (9) the variance of $\hat{\boldsymbol{Z}}$ can be written as:

$$\boldsymbol{C}_{\hat{\boldsymbol{Z}}} = [\boldsymbol{I} - \boldsymbol{M}\boldsymbol{S}] \boldsymbol{C}_{\boldsymbol{Z}} [\boldsymbol{I} - \boldsymbol{M}\boldsymbol{S}]^{\mathrm{T}} + \boldsymbol{M}\boldsymbol{C}_{\boldsymbol{W}^*} \boldsymbol{M}^{\mathrm{T}}, \tag{10}$$

where: $\boldsymbol{C}_{\boldsymbol{W}^*}$ is the diagonal block matrix of $\boldsymbol{C}_{\boldsymbol{W}_i^*}$, which is the covariance matrix of the i th measured systematic response data. Using the non-singularity property of $\boldsymbol{C}_{\boldsymbol{W}^*}$ and $\boldsymbol{C}_{\boldsymbol{Z}}$, Eq.(10) is transformed into the summation form:

$$\boldsymbol{C}_{\hat{\boldsymbol{Z}}} = \left[\boldsymbol{C}_{\boldsymbol{Z}}^{-1} + \sum_{i=1}^{n} \boldsymbol{S}_i^{\mathrm{T}} \boldsymbol{C}_{\boldsymbol{W}_i^*}^{-1} \boldsymbol{S}_i \right]^{-1}. \tag{11}$$

3. Layered shell element for the composite glass box girder

The general solid element in Fig.1 has sixteen nodes and the degraded shell element is shown in Fig. 2, whose nodal displacement vector is given as:

$$\boldsymbol{\delta}_i = [u_i \quad v_i \quad w_i \quad \beta_{1i} \quad \beta_{2i}]^{\mathrm{T}}, \tag{12}$$

where: $[u_i \quad v_i \quad w_i]^{\mathrm{T}}$ and $[\beta_{1i} \quad \beta_{2i}]^{\mathrm{T}}$ are respectively the linear displacement and the rotational displacement of node i in global coordinate system.

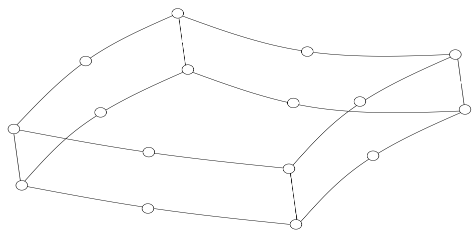

Fig. 1 General solid element

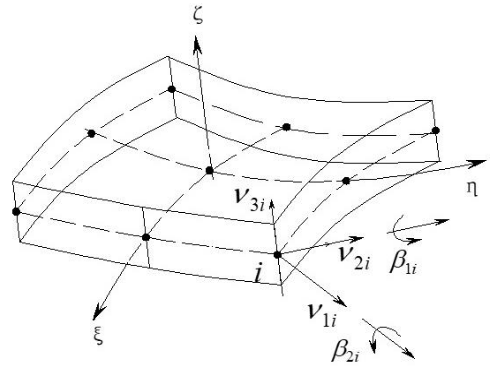

Fig. 2 Degraded shell element

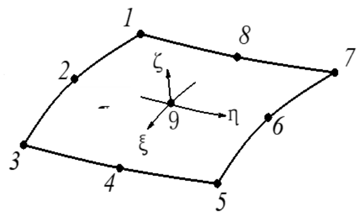

Fig. 3 Local numbers of the degraded shell element

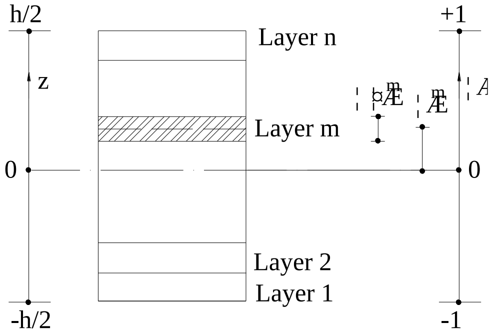

Fig. 4 Layered shell element model

The displacement fields resulted from the shape function interpolating can be expressed as:

$$u=\sum_{i=1}^{n}N_iu_i+\sum_{i=1}^{n}N_i\frac{h_i}{2}\zeta(v_{1i}^{x}\beta_{1i}-v_{2i}^{x}\beta_{2i}), \tag{13}$$

$$v=\sum_{i=1}^{n}N_iv_i+\sum_{i=1}^{n}N_i\frac{h_i}{2}\zeta(v_{1i}^{y}\beta_{1i}-v_{2i}^{y}\beta_{2i}), \tag{14}$$

$$w=\sum_{i=1}^{n}N_iw_i+\sum_{i=1}^{n}N_i\frac{h_i}{2}\zeta(v_{1i}^{z}\beta_{1i}-v_{2i}^{z}\beta_{2i}), \tag{15}$$

where: u, v and w are the displacement fields; n is the number of the nodes of the adopted element; N_i is the shape function of node i, h_i is the thickness of node i of the degraded shell element. v_{1i}^{x} is the cosine of node coordinate system $\boldsymbol{v}_{1i}$ to the x axis in the global coordinate system, v_{1i}^{y} is the cosine to y axis and v_{1i}^{z} is the cosine to z axis. v_{2i}^{x}, v_{2i}^{y} and v_{2i}^{z} can be defined by analogy. The mechanical behavior of the main material of the composite glass box girder is often discrete. In Fig. 3 and Fig. 4, the layered shell element is shown in and the internal forces are defined as:

$$S_i=\int_{-h/2}^{h/2}\sigma_i\mathrm{d}z=\frac{h}{2}\sum_{m=1}^{n}\sigma_i^m\Delta\zeta^m, \tag{16}$$

$$M_i=-\int_{-h/2}^{h/2}\sigma_i z\mathrm{d}z=-\frac{h^2}{4}\sum_{m=1}^{n}\sigma_i^m\zeta^m\Delta\zeta^m, \tag{17}$$

$$Q_i=\int_{-h/2}^{h/2}\tau_{iz}\mathrm{d}z=\frac{h}{2}\sum_{m=1}^{n}\tau_{iz}^m\Delta\zeta^m, \tag{18}$$

where: S_i, M_i and Q_i are respectively the axis force, bending moment and shearing force.

The stiffness matrix of the discussed layered shell element is gained as:

$$\boldsymbol{K}^{\mathrm{e}}=\sum_{m=1}^{n}\boldsymbol{K}_m^{\mathrm{e}}=$$
$$=\sum_{m=1}^{n}\int_{-1}^{1}\int_{-1}^{1}\int_{-1}^{1}\boldsymbol{B}_m^{\mathrm{T}}(\xi,\eta,\zeta)\boldsymbol{D}_m\boldsymbol{B}_m(\xi,\eta,\zeta)\mathrm{d}\xi\mathrm{d}\eta\mathrm{d}\zeta, \tag{19}$$

where: $\boldsymbol{B}_m$ is the strain matrix of the m th layer of the discussed layered shell element; $\boldsymbol{D}_m$ is the elastic matrix of the mth layer; $\boldsymbol{K}_m^{\mathrm{e}}$ is the stiffness matrix of the mth layer, which can be generally determined by Gaussian integral method; $\boldsymbol{K}^e$ is the stiffness matrix of the basically layered shell element [7-8]. From the layered shell element method, the solutions are provided as the theoretical results for generalized Bayesian objective function J in Eq. (4).

3. Adaptive Powell's identification method of elastic constants of composite glass box girder

3.1. Adaptive Powell's method

The two kinds of the available optimizing methods are included: the first is direct optimizing method such as simplex method, adaptive Powell's method etc and the second is gradient optimizing method such conjugate gradient method, BFGS method etc. The adaptive Powell's theory existing among the available direct optimizing methods can be regarded as an effective method, which uses a one dimensional searching method to produce the specific optimal directions from different initial searching points [22-24]. And it is independent of the partial differentiations of objective function to systematic parameters and is well suitable for the objective function without analytic expression shown in Eq. (4).

The adaptive Powell's identification steps of the elastic constants of the composite glass box girder based on generalized Bayesian objective function theory are presented as:

1. Denote $\boldsymbol{Z}^{0,0}$ as the initial values of the elastic constants $\boldsymbol{Z}$ and select $\boldsymbol{Z}^{0,0}$. Denote $\boldsymbol{b}^{0,i}$=(i=1, 2,…,m and m is the dimension of the elastic constants $\boldsymbol{Z}$) as the initial searching direction and $\boldsymbol{e}_i$ as the unit coordinate vector. Then set $\boldsymbol{b}^{0,i}=\boldsymbol{e}_i$. Give the convergence criteria ε_1 and ε_2, denote k as the iterative variable and set k=0;

2. From the elastic constants $\boldsymbol{Z}^{k,0}$, complete one dimensional searching by the optimizing direction $\boldsymbol{b}^{k,i}$ conformed to i=1, 2,…, m. It is required that $J(\boldsymbol{Z}^{k,i})=\min_h J(\boldsymbol{Z}^{k,i-1}+h\boldsymbol{b}^{k,i})$, and afterwards the systematic constant series $\boldsymbol{Z}^{k,i}$ are attained;

3. With the generalized Bayesian objective function Eq. (4), the following equation is worked out and the specific subscript l is subsequently recorded:

$$\Delta_l^k=\max_{1\le i\le m}\Delta_i^k=\max_{1\le i\le m}\left[J(\boldsymbol{Z}^{k,i-1})-J(\boldsymbol{Z}^{k,i})\right]. \tag{20}$$

4. From the elastic constants $\boldsymbol{Z}^{k,m}$, implement one dimensional optimal search by the searching direction $\boldsymbol{b}^k=\boldsymbol{Z}^{k,m}-\boldsymbol{Z}^{k,0}$, which requires that $J(\boldsymbol{Z}^{k+1,0})=\min_h J(\boldsymbol{Z}^{k,m}+h\boldsymbol{b}^k)$, and then the elastic constants

$\boldsymbol{Z}^{k+1,0}$ are achieved;

5. The convergence judgment Eqs. (21-22) is completed to judge whether the adaptive Powell's iteration convergent or not:

$$\left|J(\boldsymbol{Z}^{k+1,0})\right| < \varepsilon_1, \tag{21}$$

$$\left\|\boldsymbol{Z}^{k+1,0} - \boldsymbol{Z}^{k,0}\right\|_2 < \varepsilon_2. \tag{22}$$

If ε_1 or ε_2 is satisfied, adaptive Powell's iterative process is convergent and the identification results of the elastic constants $\boldsymbol{Z}$ are $\hat{\boldsymbol{Z}} = \boldsymbol{Z}^{k+1,0}$. The iterative process is terminated and fetch into the last step (10). If not, continue iteration;

6. Judge whether the searching direction $\boldsymbol{b}^k$ is selected. Supposing that $\boldsymbol{Z}^{k,2m}=2\boldsymbol{Z}^{k,m}-\boldsymbol{Z}^{k,0}$, the next Eq. (23) is resulted from Eq. (4) and Eq. (17):

$$\begin{aligned} J_1^k &= J(\boldsymbol{Z}^{k,0}) \\ J_2^k &= J(\boldsymbol{Z}^{k,m}) \\ J_3^k &= J(\boldsymbol{Z}^{k,2m}) \\ J_4^k &= (J_1^k - 2J_2^k + J_3^k)(J_1^k - J_2^k - \Delta_l^k)^2 \\ J_5^k &= \frac{1}{2}\Delta_l^k (J_1^k - J_3^k)^2 \end{aligned} . \tag{23}$$

If $J_3^k \geq J_1^k$, it is useless to absorb the searching direction $\boldsymbol{b}^k$. Therefore, the available searching direction is unaltered and then go into step (9). Otherwise, continue the next step;

7. If $J_4^k \geq J_5^k$, the searching direction is kept unchanged and go into step (9). If not, the calculation named absorbing the searching direction $\boldsymbol{b}^k$ is completed, in which the searching direction $\boldsymbol{b}^{k,1}$ in the available searching directions is deleted and the searching direction $\boldsymbol{b}^k$ is absorbed to replace the mth searching direction:

$$\begin{aligned} &\boldsymbol{b}^{k+1,i} = \boldsymbol{b}^{k,i}, (i = 1,2,\cdots,l-1) \\ &\boldsymbol{b}^{k+1,i} = \boldsymbol{b}^{k,i+1}, (i = l, l+1,\cdots,m-1)\,; \\ &\boldsymbol{b}^{k+1,m} = \boldsymbol{b}^k \end{aligned} \tag{24}$$

8. Let $\boldsymbol{Z}^{k,0}=\boldsymbol{Z}^{k+1,0}$, $\boldsymbol{b}^{k,i}=\boldsymbol{b}^{k+1,i}$, $k=k+1$ and go back to step (2) to continue iterating;

9. Let $\boldsymbol{Z}^{k,0}=\boldsymbol{Z}^{k+1,0}$, $k=k+1$ and go back to step (2) to continue iterating;

10. From Eq. (11), the covariance $\boldsymbol{C}_{\hat{\boldsymbol{Z}}}$ of the elastic constants $\boldsymbol{Z}$ is achieved.

3.2. Determination of the optimal step length

Among the available achievements, the one dimensional searching methods are mainly referred to golden sectional method, quadratic parabolic interpolation method, etc. During these methods, quadratic parabolic interpolation method has much satisfying computational efficiency, automatically determining the span the optimal step length h lies in and then optimizing the step length. The main steps include:

1. Denote the initial step length as h_1 and a step length increment as h_0. Set h_0, h_1 and compute $h_2 = h_1 + h_0$. If $J(h_1) \geq J(h_2)$, the step length increment is calculated, which is defined as $h_k = h_{k-1} + 2^{k-2}h_0$ where $k \geq 3$. The calculation continues until $J(h_k) \geq J(h_{k-1})$. If $J(h_1) < J(h_2)$, the other step length increment is calculated, which is defined as $h_k = h_{k-1} - 2^{k-3}h_0$ where $k \geq 3$. The calculation continues until $J(h_k) \geq J(h_{k-1})$.

The range of h called the optimal step length is obtained and noted as $[h_a, h_d]$ when the iterative calculation is terminative.

2. From the function extremum theory of the generalized Bayesian objective function, h called the optimal step length is achieved:

$$h = \frac{1}{2}(h_a + h_d - \frac{h_b}{h_c}), \tag{25}$$

$$h_b = \frac{J(h_d) - J(h_a)}{h_d - h_a}, \tag{26}$$

$$h_c = \frac{1}{h_e - h_d}\left[\frac{J(h_e) - J(h_a)}{h_e - h_a} - h_b\right], \tag{27}$$

where: h_a and h_d are the values of the two endpoints of the span where h lies; h_b and h_c are both the transitional variables; h_e is the mid-point of the range $[h_a, h_d]$.

4. Analysis of typical examples

The adaptive Powell's identification of elastic constants defined as $\boldsymbol{E} = [E_1\ E_2\ E_3]^{\mathrm{T}}$ of the composite glass box girder shown in Fig.5 is studied in this paper, where E_1, E_2 and E_3 are respectively the Young's modulus of the top plate, abdomen plate and bottom plate [12-13]. The numbers of the layered shell elements and the nodes of the support section plane of the composite glass box girder are shown in Fig. 5 and the others can be got by recursion along the longitude direction.

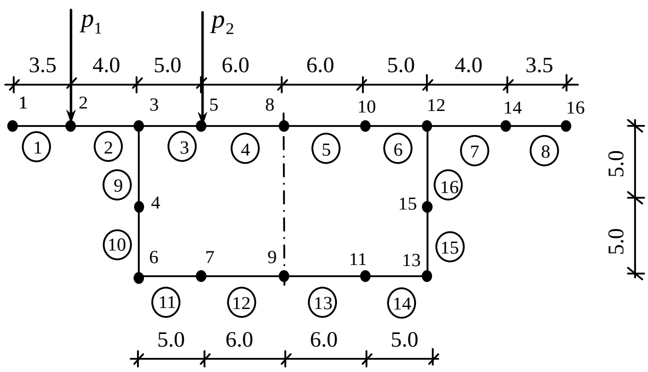

Fig. 5 Element subdivision of the composite glass box girder /cm

The length of the composite glass box girder is 120 cm. The widths of the top plate, abdomen plate and bottom plate recorded as t_1, t_2 and t_3 are listed in Table 1. The true values of the elastic constants $\boldsymbol{E}$ and Poisson's ratio μ are also in Table1 and the variation coefficient is supposed as 0.1. The vertical uniform loads p_1=4 N/cm and p_2=8 N/cm are respectively added to the node of No. 2 and 5 of the composite glass box girder along the longitude direction. The five points from No. 1 to No. 5 in the mid-span section plane are selected as displacement measured points and the displacements of every point are measured for five times whose expectations and standard variances of the measured displacements are listed in Table 2. For putting the adaptive Powell's identification of the elastic constants of the composite glass box girder into practice, the identification procedure is developed, in which the subroutine procedure proved for the mechanical analysis of the composite glass box girder is employed [7-8].

Table 1

True values of elastic constants and Poisson's ratio and the widths of the box

Parameter's name	t_1, cm	t_2, cm	t_3, cm	E_{1true}, 10^4N/cm^2	E_{2true}, 10^4N/cm^2	E_{3true}, 10^4N/cm^2	μ
Value	0.50	0.45	0.50	300	200	350	0.17

Table 2

The measured displacements and standard variances

Selected points	Displacement expectations w, cm					Displacement standard variances σ_w, cm				
	w_1	w_2	w_3	w_4	w_5	σ_{W_1}	σ_{W_2}	σ_{W_3}	σ_{W_4}	σ_{W_5}
1	0.035	0.037	0.032	0.033	0.038	0.051	0.055	0.054	0.056	0.048
2	0.032	0.036	0.034	0.034	0.037	0.062	0.066	0.067	0.063	0.060
3	0.033	0.038	0.031	0.032	0.034	0.043	0.041	0.047	0.040	0.045
4	0.032	0.031	0.036	0.034	0.036	0.040	0.042	0.043	0.046	0.042
5	0.041	0.044	0.045	0.040	0.044	0.059	0.053	0.055	0.051	0.056

Case 1. Adaptive Powell's identification of the elastic constants of the composite glass box girder when the priori information is precise, meaning that the priori information of the box girder is supposed to satisfy the precise condition and here equal to the true values. For carrying out the adaptive Powell's identification, select the initial values of the elastic constants $\boldsymbol{E}_{1,0}=[450.0, 300.0, 525.0]^T$ and $\boldsymbol{E}_{2,0}=[150.0, 100.0, 175.0]^T$ respectively and the deviation degrees from the true values are all 50 %. The convergence criteria is supposed as ε_1=0.001, ε_2=0.001, which are put into the adaptive Powell's identification procedure with the data shown in Table 2. And the iterative results of the elastic constants are achieved in Table 3 and Fig. 6.

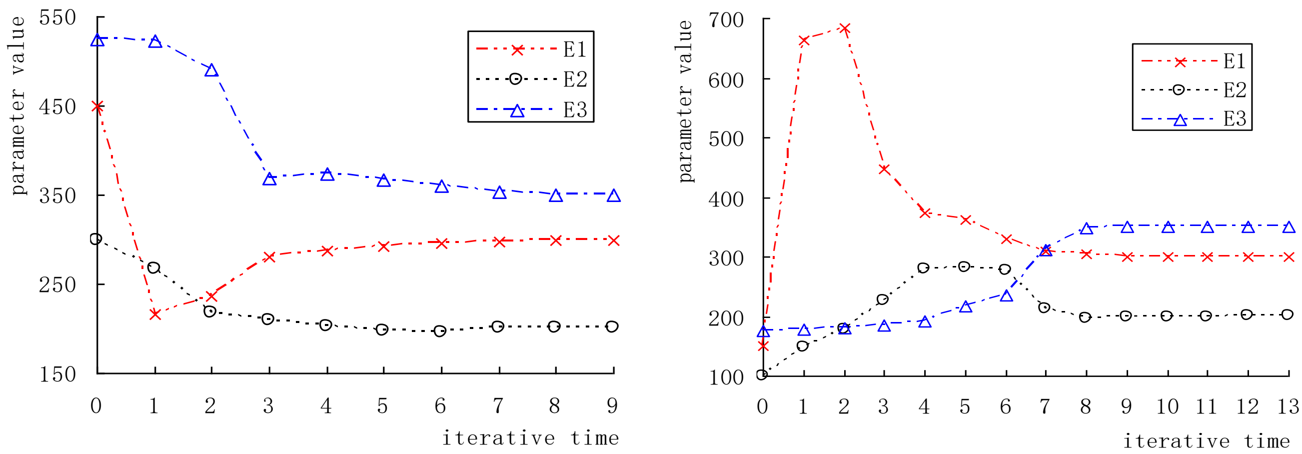

a) Iterative results of $\boldsymbol{E}_{1,0}$ b) Iterative results of $\boldsymbol{E}_{2,0}$

Fig. 6 Iterative results of the elastic constants of the composite glass box structure in Case 1/ (10^4 N/cm^2)

Table 3

Results of adaptive Powell's identification of elastic constants of composite glass box structure in Case 1

Elastic constants	E_1, 10^4N/cm^2	E_2, 10^4N/cm^2	E_3, 10^4N/cm^2	E_1, 10^4N/cm^2	E_2, 10^4N/cm^2	E_3, 10^4N/cm^2
Initial value	450.0	300.0	525.0	150.0	100.0	175.0
Final value	299.73	200.65	349.75	299.89	200.25	350.04
Iterative times	9	9	9	13	13	13
Relative error, %	0.09	0.32	0.07	0.04	0.12	0.01
Convergent criterion	ε_1	ε_1	ε_1	ε_2	ε_2	ε_2

From the results in Table 3 and Fig. 5, it is indicated that if the priori information is precise, the iterative process of the adaptive Powell's identification of elastic constants of the composite glass box girder is steadily convergent to the true constant values, which is independent of the initial constant values. And in conformity to ε_1 and ε_2, the processes of the iterations can both be convergent. The identification efficiency is determined by many factors but mostly determined by the times that the subroutine procedure of the layered shell element analysis for the composite glass box girder is called. From a great deal of computations and in comparison with the achievements [12-13], adaptive Powell's theory is impertinent with the partial differentiation of the systematic responses from the layered shell element analysis to the elastic constants and there is unnecessary to call the layered shell element analysis procedure for extra times, which evidently proves higher efficiency of the deduced adaptive Powell's method.

Case 2. For obtaining some other regularities of the adaptive Powell's identification of the elastic constants of the composite glass box structure when the priori information is precise, the initial values of elastic constants $\boldsymbol{E}_{3,0}=[525.0, 525.0, 525.0]^{\mathrm{T}}$ and $\boldsymbol{E}_{4,0}=[100.0, 100.0, 100.0]^{\mathrm{T}}$ are respectively selected. $\boldsymbol{E}_{3,0}$ and $\boldsymbol{E}_{4,0}$ are farther from the true values compared with $\boldsymbol{E}_{1,0}$ and $\boldsymbol{E}_{2,0}$. The rest data are the same as Case 1 and from the developed procedure, the iterative results are achieved in Table 4 and Fig. 7.

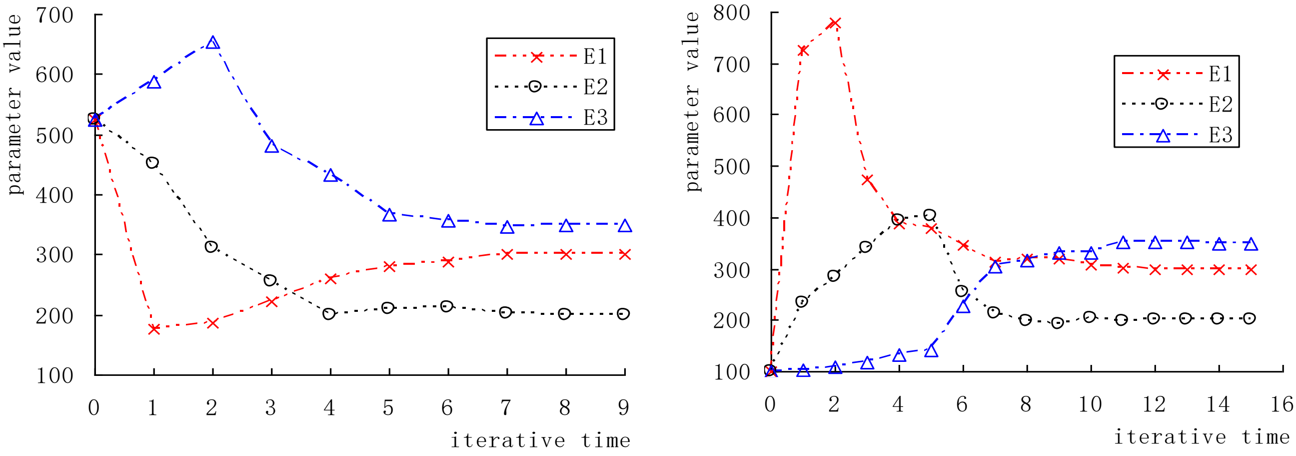

a) Iterative results of $\boldsymbol{E}_{3,0}$ b) Iterative results of $\boldsymbol{E}_{4,0}$

Fig. 7 Iterative results of the elastic constants of the composite glass box structure in Case 2/ (10^4 N/cm^2)

Table 4

Results of adaptive Powell's identification of elastic constants of composite glass box structure in Case 2

Elastic constants	E_1, 10^4N/cm^2	E_2, 10^4N/cm^2	E_3, 10^4N/cm^2	E_1, 10^4N/cm^2	E_2, 10^4N/cm^2	E_3, 10^4N/cm^2
Initial value	525.0	525.0	525.0	100.0	100.0	100.0
Final value	299.99	200.26	349.69	299.98	200.27	350.09
Iterative times	9	9	9	15	15	15
Relative error, %	0.002	0.13	0.09	0.01	0.14	0.03
Convergent criterion	ε_2	ε_2	ε_2	ε_1	ε_1	ε_1

From Table 4 and Fig. 7, it is shown that the iterative times cannot get fewer when the convergence criterion is satisfied and the convergence precision cannot yet become higher when the initial constant values approach closer to the true values in the identification of the poly constants. The reason leading to the regularity lies in that during the identification processes of the poly constants, the relationships between the poly constants are interactional and interdependent.

Case 3. Adaptive Powell's identification of elastic constants of composite glass box girder when the priori information is imprecise. Let priori information $\boldsymbol{E}_0=[400.0, 400.0, 400.0]^{\mathrm{T}}$. In order to make comparison conveniently, let initial constant values

$\boldsymbol{E}_{1,0}=[450.0, 300.0, 525.0]^{\mathrm{T}}$ and $\boldsymbol{E}_{2,0}=[150.0, 100.0, 175.0]^{\mathrm{T}}$.

The iterative results of adaptive Powell's identification of elastic constants are achieved in Table 5 when the other data are the same as Case 1. The relative fluctuation degree of parameters is shown in Table 6.

Table 5

Results of adaptive Powell's identification of elastic constants of the composite glass box girder in Case 3

Elastic constants	E_1, 10^4N/cm^2	E_2, 10^4N/cm^2	E_3, 10^4N/cm^2	E_1, 10^4N/cm^2	E_2, 10^4N/cm^2	E_3, 10^4N/cm^2
Initial value	450.0	300.0	525.0	150.0	100.0	175.0
Final value	404.32	277.28	428.67	121.36	126.19	214.86
Iterative times	14	14	14	100	100	100
Relative error η, %	34.77	10.91	22.48			
Convergent criterion	ε_2	ε_2	ε_2	divergent	divergent	divergent

Table 6

Relative fluctuating degree of iterative results by different groups of initial values

Elastic constants	E_1, 10^4N/cm^2	E_2, 10^4N/cm^2	E_3, 10^4N/cm^2	E_1, 10^4N/cm^2	E_2, 10^4N/cm^2	E_3, 10^4N/cm^2
Pre-known value	300.0	200.0	350.0	400.0	400.0	400.0
Final value $E_{1,e}$	299.99	200.26	349.69	404.32	277.28	428.67
Final value $E_{2,e}$	299.98	200.27	350.09	415.03	262.69	454.24
Relative fluctuating degree ζ, %	0.003	0.005	0.114	2.614	5.404	5.792

Note: $\xi = 2|E_{1,e} - E_{2,e}|/(E_{1,e} + E_{2,e}) \times 100\%$

From Table 5, It can be found that the parameter iteration process sometimes converges and sometimes diverges, which indicates that the parameter cannot converge steadily to the actual value of the parameter. Even if the iteration process can converge, the relative errors of parameters are larger, all exceeding 5 %. When the prior information is inaccurate, if the iteration process converges, it can only converge according to the second criterion. Secondly from Table 6, with comparison of that the prior information is accurate, the relative fluctuation degree of parameters will be greater when convergence occurs.

5. Conclusions

1. The adaptive Powell's identification of elastic constants of the composite glass box girder is steadily convergent to the true constant values when the priori information is precise which shows that the derived identification model is correct and reliable.

2. In comparison with gradient optimization method, the adaptive Powell's method is irrelevant with the partial differentiation of the systematic responses from the layered shell element analysis to the elastic constants, which evidently proves higher efficiency of the derived adaptive Powell's method.

3. In the identification of the poly constants, the iterative times cannot always get fewer when the initial constant values approach closer to the true values and the convergence criterion is satisfied. The reason is that during the processes of the identification of the poly constants, the relations between the poly constants are interdependent and interactional.

Acknowledgements

This project is supported by the Fundamental Research Funds for the Central Universities (NO. NS2020009).

References

1. **Alexandre, C.; Christian, C.; John, D.** 2012. Long-term monitoring of a PSC composite glass box girder bridge: operational modal analysis, data normalization and structural modification assessment, Mechanical Systems and Signal Processing 33(11): 13-37. http://dx.doi.org//10.1016/j.ymssp.2012.07.005.
2. **Nanthakumar, S. S.; Lahmer, T.; Zhuang, X.** et al. 2016. Detection of material interfaces using a regularized level set method in piezoelectric structures, Inverse Problems in Science and Engineering 24(1):153-176. http://dx.doi.org//10.1080/17415977.2015.1017485.
3. **Nanthakumar, S. S.; Lahmer, T.; Rabczuk, T.** 2013. Detection of flaws in piezoelectric structures using XFEM, International Journal of Numerical Methods in Engineering 96(6):373-389. http://dx.doi.org//10.1016/j.cma.2014.03.001.
4. **Robert, K D.; Timothy, P. J.** 2012. Closed-form shear flow solution for box–girder bridges under torsion, Engineering Structures 34(1): 383-390. http://dx.doi.org//10.1016/j.engstruct.2011.09.023.
5. **Belabed, Z.; Houari, M. S. A.; Tounsi, A**. et al. 2014. An efficient and simple higher order shear and normal deformation theory for functionally graded material (FGM) plates, Composites: Part B 60(3): 274-283. http://dx.doi.org//10.1051/meca/2015112.
6. **Xia, G. Y.; Zeng, Q. Y.; Li, C. X.** et al. 2004. Thick/thin plate rectangular element based on finite strip, Mechanics in Engineering 26(6): 51-55. http://dx.doi.org//10.6052/1000-0992-2003-372.
7. **Bourada, M.; Kaci, A.; Houari, M. S. A.** et al. 2015. A new simple shear and normal deformations theory for functionally graded beams, Steel and Composite Structures 18(2): 409-423. http://dx.doi.org//10.12989/scs.2015.18.2.409.
8. **Hamdia, K. M.; Silani, M.; Zhuang, X. Y.** et al. 2017. Stochastic analysis of the fracture toughness of polymericnanoparticle composites using polynomial chaos expansions, International Journal of Fracture 206: 215-227. http://dx.doi.org/10.1007/s10704-017-0210-6.
9. **He, X. H.; Sheng, X. W.; Scanlon, A.** et al. 2012. Skewed concrete composite glass box girder bridge static and dynamic testing and analysis, Engineering Structures 39(6): 38-49. http://dx.doi.org//10.1016/j.engstruct.2012.01.016.
10. **Larson, K. H.; Peterman, R. J.; Rasheed, H. A.** 2005. Strength-fatigue behavior of fiber reinforced polymer strengthened prestressed concrete T-beams, Journal of Composites for Construction 9(4): 313-326. http://dx.doi.org//10.1061/(asce)1090-0268(2005)9:4(313).
11. **Hamdia, K. M.; Ghasemi, H.; Zhuang, X. Y.** et al. 2018. Sensitivity and uncertainty analysis for flexoelectric nanostructures, Computer Methods in Applied Mechanics and Engineering 337, 95-109. https://doi.org/10.1016/j.cma.2018.03.016.
12. **Khader, M. H.; Zhuang, X. Y.; He, P. F.** et al. 2016. Fracture toughness of polymeric particle nanocomposites: evaluation of models performance using Bayesian method, Composite Science and Technology 126(4): 122-129. http://dx.doi.org//10.1016/j.compscitech.2016.02.012.
13. **Zhang, J.; Ye, J. S.; Zhao, X. M.** 2007. Dynamic Bayesian estimation of displacement parameters of continuous curve box based on Novozhilov theory, Applied Mathematics and Mechanics 28(1): 87-95. http://dx.doi.org//10.1007/s10483-007-0110-z.
14. **Wen, Q. J.** 2011. Long-term effect analysis of prestressed concrete box-girder bridge widening, Construction and Building Materials 25(4): 1580-1586. http://dx.doi.org//10.1016/j.conbuildmat.2010.09.041.
15. **Zhang, J.; Ye, J. S.; Wang, C. Q.** 2008. Dynamic Bayesian estimation of displacement parameters of continuous thin walled straight box with segregating slab based on CG method, Chinese Journal of Computational Mechanics 25(4): 574-580. http://dx.doi.org//10.1007/s10870-007-9222-9.
16. **Li, T. C.; Lyu, L. X.; Zhang, S. L.** et al. 2015. Development and application of a statistical constitutive model of damaged rock affected by the load-bearing capacity of damaged elements, Journal of Zhejiang University-SCIENCE A (Applied Physics & Engineering) 16(8): 644-655. http://dx.doi.org//10.1631/jzus.A1500034.
17. **Jia, Y. F.; Chi, S. C.** 2015. Back-analysis of soil parameters of the Malutang II concrete face rockfill dam

using parallel mutation particle swarm optimization, Computers and Geotechnics 65(4):87-96. http://dx.doi.org//10.1016/j.compgeo.2014.11.013.

18. **Arsava, K. S.; Nam, Y. Y.; Kim, Y.** 2016. Nonlinear system identification of smart reinforced concrete structures under impact loads, Journal of Vibration and Control 22(16): 3576-3600. http://dx.doi.org//10.1177/1077546314563966.
19. **Xie, Y. F.** 2011. Least square inversed analysis of soil parameter for foundation with two-order gradient theoretic method, Advanced Materials Research 243-249: 2294-2299. http://dx.doi.org//10.4028/www.scientific.net/AMR.243-249.2294.
20. **Bousahla, A. A.; Houari, M. S. A.; Tounsi, A.** et al. 2014. A novel higher order shear and normal deformation theory based on neutral surface position for bending analysis of advanced composite plates, International Journal of Computational Methods 11(6): 19-30. http://dx.doi.org//10.1142/S0219876213500825.
21. **Bouderba, B.; Houari, M. S. A.; Tounsi, A.** 2013. Thermomechanical bending response of FGM thick plates resting on Winkler-Pasternak elastic foundations, Steel and Composite Structures 14(1): 85-104. http://dx.doi.org//10.12989/scs.2013.14.1.085.
22. **Zidi, M.; Tounsi, A. ; Houari, M. S. A.** et al. 2014. Bending analysis of FGM plates under hygro-thermo-mechanical loading using a four variable refined plate theory, Aerospace Science and Technology 34(4): 24-34. http://dx.doi.org//10.1016/j.ast.2014.02.001.
23. **Vu-Bac, N.; Lahmer, T. ; Zhuang, X.** et al. 2016. A software framework for probabilistic sensitivity analysis for computationally expensive models, Advances in Engineering Software 100: 19-31. http://dx.doi.org/10.1016/j.advengsoft.2016.06.005.
24. **Ait, A. M.; Hadj, H. A.; Abdelouahed, T.** 2014. An efficient and simple refined theory for buckling and free vibration of exponentially graded sandwich plates under various boundary conditions, Journal of Sandwich Structures and Materials 16(3):293-318. http://dx.doi.org//10.1177/1099636214526852.

J. Zhang, Y. L. Jiang, W. Sun, H. Liu, G. D. Li, J.Y. Wang

ADAPTIVE POWELL’S IDENTIFICATION OF ELASTIC CONSTANTS OF COMPOSITE GLASS GIRDER WITH LAYERED SHELL ELEMENT THEORY

S u m m a r y

For the composite glass box girder, the generalized Bayesian objective function of elastic constants of the structure was derived based on layered shell element theory. Mechanical performances of the composite glass box girder were solved by layered shell element method. Combined with quadratic parabolic interpolation search scheme of optimized step length, the adaptive Powell’s optimization theory was taken to complete the stochastic identification of elastic constants of composite glass box girder. Then the adaptive Powell’s identification steps of elastic constants of the structure were presented in detail and the adaptive Powell’s identification procedure was accomplished. From some classic examples, it is finally achieved that the adaptive Powell’s identification of elastic constants of composite glass box girder has perfect convergence and numerical stability, which testifies that the adaptive Powell’s identification theory of elastic constants of composite glass box girder is correct and reliable. The stochastic characteristics of systematic responses and elastic constants are well deliberated in generalized Bayesian objective function. And in iterative processes, the adaptive Powell’s identification is irrelevant with the complicated partial differentiation of the systematic responses from the layered shell element model to the elastic constants, which proves high computation efficiency.

Keywords: adaptive Powell’s theory; identification; generalized Bayesian theory; composite glass box girder; elastic constants.

Received September 25, 2019
Accepted October 14, 2020